CrystEngComm

PAPER

View Article Online
View Journal | View Issue

Cite this: *CrystEngComm*, 2016, **18**, 2650

Exploration of Cd(II)/pseudohalide/di-2-pyridyl ketone chemistry – rational synthesis, structural analysis and photoluminescence†

I. Nawrot,[a] B. Machura*[a] and R. Kruszynski[b]

Received 15th January 2016,
Accepted 27th February 2016

DOI: 10.1039/c6ce00112b

www.rsc.org/crystengcomm

A systematic investigation of Cd(II)–$(py)_2CO$–X systems (X = N_3^-, NCO^- and NCS^-) was conducted, and the following cadmium(II) coordination compounds $[Cd(SCN)_2\{(py)_2C(OCH_3)(OH)\}]_n$ (**1**), $[Cd_2(SCN)_4\{(py)_2C(OCH_3)(OH)\}_2]$ (**2**), $[Cd_4(SCN)_4\{(py)_2C(OCH_3)(O)\}_4]$ (**3**), $[Cd_4(N_3)_4\{(py)_2C(OCH_3)(O)\}_4]$ (**4**), $[Cd_4(N_3)_4\{(py)_2C(OH)(O)\}_2\{(py)_2C(OCH_3)(O)\}_2]$ (**5**), $[Cd_4(NCO)_4\{(py)_2C(OCH_3)(O)\}_4]$ (**6**), $[Cd_4(NCO)_4\{(py)_2C(OH)(O)\}_2\{(py)_2C(OCH_3)(O)\}_2]$ (**7**), $[Cd_4(N_3)_2(NO_3)_2\{(py)_2C(OH)(O)\}_2\{(py)_2C(OCH_3)(O)\}_2]$ (**8**) and $[Cd_4(NCO)_2(NO_3)_2\{(py)_2C(OH)(O)\}_2\{(py)_2C(OCH_3)(O)\}_2]$ (**9a** and **9b**) were successfully synthesized and characterized by single-crystal diffraction, X-ray powder diffraction (XRPD), differential scanning calorimetry (DSC) analysis and IR spectroscopy. The fluorescence properties of **1**–**9** were studied in the solid state and compared to the fluorescence of di-2-pyridyl ketone. The photoluminescence behaviour of **2**–**9** was also investigated in acetonitrile solution. The X-ray studies demonstrated a cooperative impact of the organic ligand and auxiliary inorganic ion on the final molecular architectures of the cadmium(II) coordination compounds. Also, the essential roles of intermolecular interactions (hydrogen bonds, π–π stacking interactions and weak O···S contacts) in the creation of molecular architectures were discussed.

Introduction

The di-2-pyridyl ketone $[(py)_2CO]$ with three potential donor sites is a versatile polydentate ligand whose reactions with transition metal and lanthanide ions have been extensively studied since 1967, when Osborne and McWhinnie reported the first Cu(II) complexes of $(py)_2CO$.[1]

Initially, it was thought that $(py)_2CO$ had the ability to coordinate to a metal ion as a tridentate ligand with bonding through the oxygen and two nitrogen atoms or in a bidentate way through the two nitrogen atoms located in the pyridine rings or through one pyridyl nitrogen and the carbonyl oxygen.[2]

Further studies demonstrated that the ketocarbonyl group of $(py)_2CO$ undergoes metal-promoted solvation (H_2O, ROH) which yields the *gem*-diol form $(py)_2C(OH)_2$ or hemiketal form $(py)_2C(OR)(OH)$ (Scheme 1), coordinating to the metal centres usually in a tridentate way *N*,*N*′,*O*, with the M–O bond often being weak.

The solvation process is accounted for the steric strain on the carbonyl carbon produced upon complexation. It is thought that the conversion of the sp^2 hybridized C atom in $(py)_2CO$ to sp^3 $(py)_2C(OH)_2$ and $(py)_2C(OR)(OH)$ is facilitated by metals in high oxidation states. Complexes with low oxidation state transition metals (Ag^+) usually contain the ketone form $(py)_2CO$.[3]

Interesting coordination modes are also seen when the ligands $(py)_2C(OH)_2$ and $(py)_2C(OR)(OH)$ become deprotonated. The monoanionic forms usually bridge two (μ_2) or three (μ_3) metal ions, while the dianionic form can bridge up to five metal sites (μ_5) (Scheme 2) yielding various polynuclear

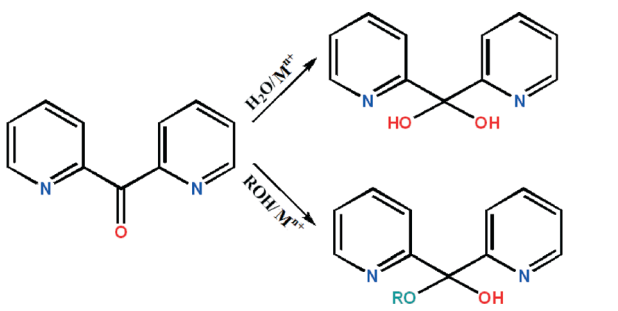

Scheme 1 Di-2-pyridyl ketone together with its *gem*-diol and hemiketal forms.

[a] *Department of Crystallography, Institute of Chemistry, University of Silesia, 9th Szkolna St., 40-006 Katowice, Poland. E-mail: basia@ich.us.edu.pl*
[b] *Department of X-ray Crystallography and Crystal Chemistry, Institute of General and Ecological Chemistry, Technical University of Lodz, 116 Żeromski St., 90-924 Łódź, Poland. E-mail: rafal.kruszynski@p.lodz.pl*

† Electronic supplementary information (ESI) available: Experimental and calculated XRPD spectra, IR spectra, DSC curves, electronic absorption spectra in the solid state and in acetonitrile solution. CCDC 1446466–1446474. For ESI and crystallographic data in CIF or other electronic format see DOI: 10.1039/c6ce00112b

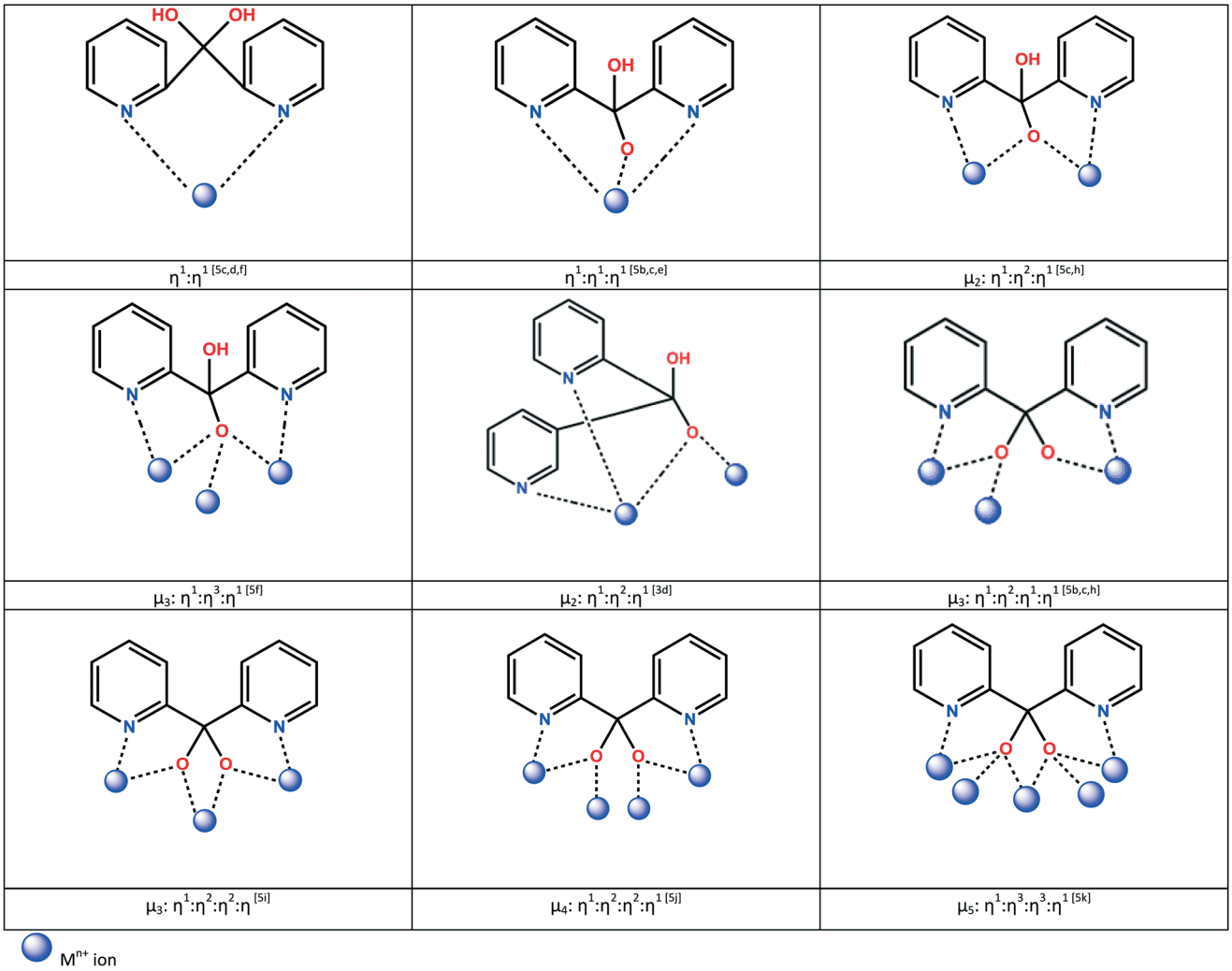

Scheme 2 Bridging coordination modes of $(py)_2C(OH)O^-$ and $(py)_2CO_2^{2-}$.

compounds of high significance in molecular magnetism and catalysis.[4] Among these, special attention has been paid to the cubane-like structures of tetranuclear metal complexes.[5]

Although the use of $(py)_2CO$ has been investigated widely in Mn, Fe, Co, Ni, Cu and Zn chemistry,[6] its employment in the synthesis of cadmium(II) compounds is rather limited. A search in the CSD (Cambridge Structural Database, version 5.36) revealed only a few Cd(II) compounds incorporating $(py)_2CO$ or its derivatives: $[Cd_2Cl_4\{(py)_2C(OH)(OH)\}_2]\cdot 3H_2O$,[7] $[Cd_2Br_4\{(py)_2C(OH)(OH)\}_2]\cdot 3H_2O$,[8] $[Cd_2I_4\{(py)_2C(OMe)(OH)\}_2]$,[9] $[Cd_2(NO_3)_4\{(py)_2CO\}_2]$,[5h] $[Cd_4(NO_3)_4\{(py)_2C(OH)(O)\}_4]$[5h] and $[Cd_4(SCN)_4\{(py)_2C(OMe)(O)\}_4]$.[5d]

Following the well-known strategy of combining the use of heterocyclic organic blockers and pseudohalide ions in the synthesis of coordination compounds, we have conducted a systematic investigation of Cd(II)–$(py)_2CO$–X systems ($X = N_3^-$, NCO^- and NCS^-). By changing the anions, M : X molar ratio or reaction conditions, we have isolated a series of new pseudohalide Cd(II) compounds $[Cd(SCN)_2\{(py)_2C(OCH_3)(OH)\}]_n$ (**1**), $[Cd_2(SCN)_4\{(py)_2C(OCH_3)(OH)\}_2]$ (**2**), $[Cd_4(SCN)_4\{(py)_2C(OCH_3)(O)\}_4]$ (**3**), $[Cd_4(N_3)_4\{(py)_2C(OCH_3)(O)\}_4]$ (**4**), $[Cd_4(N_3)_4\{(py)_2C(OH)(O)\}_2\{(py)_2C(OCH_3)(O)\}_2]$ (**5**), $[Cd_4(NCO)_4\{(py)_2C(OCH_3)(O)\}_4]$ (**6**), $[Cd_4(NCO)_4\{(py)_2C(OH)(O)\}_2\{(py)_2C(OCH_3)(O)\}_2]$ (**7**),

$[Cd_4(N_3)_2(NO_3)_2\{(py)_2C(OH)(O)\}_2\{(py)_2C(OCH_3)(O)\}_2]$ (**8**) and $[Cd_4(NCO)_2(NO_3)_2\{(py)_2C(OH)(O)\}_2\{(py)_2C(OCH_3)(O)\}_2]$ (**9a** and **9b**), which were structurally characterized by single crystal X-ray diffraction analysis and further characterized by infrared spectroscopy (IR), elemental analyses, X-ray powder diffraction (XRPD) and differential scanning calorimetry (DSC) analyses. The X-ray studies demonstrated a cooperative impact of the organic ligand and auxiliary inorganic ion on the final molecular architectures of cadmium(II) coordination compounds. An essential role of intermolecular interactions (hydrogen bonds, π–π stacking interactions and weak O···S contacts) in the creation of molecular architectures was also proven. The luminescence properties of di-2-pyridyl ketone and cadmium(II) coordination compounds were studied in solution and the solid state.

Experimental section

Synthetic procedures

General. The reagents used in the synthesis were commercially available (POCH and Aldrich) and they were used without further purification.

Synthesis of $[Cd(SCN)_2\{(py)_2C(OCH_3)(OH)\}]_n$ (1). NH_4SCN (0.10 g, 1.3 mmol) dissolved in methanol (15 mL) was added to the methanolic solution (35 mL) of $Cd(NO_3)\cdot 4H_2O$ (0.2 g, 0.65 mmol) and $(py)_2CO$ (0.12 g, 0.65 mmol) and refluxed for 4 h. After cooling to room temperature, the resulting colourless solution was filtered to remove any small particle and left to evaporate in a hood at room temperature. Crystals of 1 as white plates suitable for X-ray analysis were formed after two weeks and they were collected and dried in the open air. Yield 80% (based on Cd). Anal. calc. for $C_{14}H_{12}CdN_4O_2S_2$: C, 37.80; H, 2.72; N, 12.60%. Found: C, 37.59; H, 2.66; N, 12.43%. Selected IR data (KBr; cm^{-1}): 3225(s), 2115(vs), 2087(vs), 1601(s), 1575(m), 1467(m), 1441(s), 1384(m), 1269(m), 1202(m), 1159(s), 1090(s), 1047(s), 1018(m), 939(m), 796(s), 758(s), 678(m), 641(m), 520(m) and 460(m). UV–vis (solid state; λ_{max} [nm]): 370, 265.

Synthesis of $[Cd_2(SCN)_4\{(py)_2C(OCH_3)(OH)\}_2]$ (2). NH_4SCN (0.10 g, 1.3 mmol) dissolved in methanol (15 mL) was added to the methanolic solution (35 mL) of $Cd(NO_3)\cdot 4H_2O$ (0.2 g, 0.65 mmol) and $(py)_2CO$ (0.12 g, 0.65 mmol) and the resulting colourless solution was stirred at room temperature for 12 h. It was filtered to remove any small particle and left to evaporate in a hood at room temperature. Crystals of 2 as white polyhedrons suitable for X-ray analysis formed after a few days and they were collected and dried in the open air. Yield 70%. Anal. calc. for $C_{28}H_{24}Cd_2N_8O_4S_4$: C, 37.80; H, 2.71; N, 25.55%. Found: C, 37.28; H, 2.65; N, 25.15%. Selected IR data (KBr, cm^{-1}): 3110(s, br), 2126(vs), 2100(vs), 1600(s), 1574(m), 1467(m), 1440(s), 1385(m), 1307(m), 1271(m), 1241(m), 1210(m), 1164(s), 1091(m), 1037(s), 1016(s), 943(m), 794(s), 770(s), 641(m), 523(m) and 460(m). UV–vis (solid state; λ_{max} [nm]): 369, 265 and 222. UV–vis (MeCN; λ_{max} [nm] (ε; $dm^3\ mol^{-1}\ cm^{-1}$)): 350 (383), 271 (79 390) and 235 (98 340).

Synthesis of $[Cd_4(SCN)_4\{(py)_2C(OCH_3)(O)\}_4]$ (3). NH_4SCN (0.05 g, 0.65 mmol) dissolved in methanol (15 mL) was added to the methanolic solution (35 mL) of $Cd(NO_3)\cdot 4H_2O$ (0.2 g, 0.65 mmol) and $(py)_2CO$ (0.12 g, 0.65 mmol) and the resulting solution was stirred at room temperature for 6 h. It was filtered to remove any small particle and left to evaporate at room temperature. After a few days, a white crystalline precipitate of 3 was collected in 40% yield. Compound 3 has been previously reported.[5d]

Synthesis of $[Cd_4(N_3)_4\{(py)_2C(OCH_3)(O)\}_4]$ (4). The same synthetic procedure as that for 1 was used except that ammonium thiocyanate was replaced with sodium azide (0.085 g, 1.3 mmol). A white crystalline precipitate of 4 was collected in 60% yield. Anal. calc. for $C_{48}H_{44}Cd_4N_{20}O_8$: C, 38.99; H, 3.00; N, 18.95%. Found: C, 48.38; H, 2.87; N, 18.59%. Selected IR data (KBr; cm^{-1}): 2048(vs), 2039(sh), 1600(s), 1541(m), 1467(m), 1437(s), 1336(m), 1303(m), 1264(w), 1236(m), 1209(m), 1113(m), 1094(s), 1070(s), 1056(m), 1013(m), 959(w), 906(m), 795(m), 781(s), 759(m), 686(m), 638(m), 468(m), 436(w). UV–vis (solid state; λ_{max} [nm]): 445, 385 and 269. UV–vis (MeCN; λ_{max} [nm] (ε; $dm^3\ mol^{-1}\ cm^{-1}$)): 378 (1011), 275 (97 550).

Synthesis of $[Cd_4(N_3)_4\{(py)_2C(OH)(O)\}_2\{(py)_2C(OCH_3)(O)\}_2]$ (5). The synthetic procedure was similar to that of 2, except that ammonium thiocyanate was replaced with sodium azide (0.085 g, 1.3 mmol). White crystals of 5 were obtained in 65% yield. Anal. calc. for $C_{48}H_{44}Cd_4N_{20}O_8$: C, 38.09; H, 2.78; N, 19.31%. Found: C, 38.45; H, 2.69; N, 19.57%. Selected IR data (KBr; cm^{-1}): 3379(br), 2064(vs), 2036(vs), 1598(s), 1570(m), 1468(m), 1436(s), 1385(m), 1334(m), 1264(m), 1228(m), 1130(m), 1113(m), 1088(m), 1048(s), 1016(m), 954(m), 788(m), 774(m), 752(m), 680(m), 635(m), 457(m), 436(m). UV–vis (solid state; λ_{max} [nm]): 449, 262 and 221. UV–vis (MeCN; λ_{max} [nm] (ε; $dm^3\ mol^{-1}\ cm^{-1}$)): 358 (618), 267 (61 650) and 233 (69 460).

Synthesis of $[Cd_4(NCO)_4\{(py)_2C(OCH_3)(O)\}_4]$ (6). The same synthetic procedure as that for 1 was used except that ammonium thiocyanate was replaced with sodium cyanate (0.085 g, 1.3 mmol). White crystals of 6 were obtained in 70% yield. Anal. calc. for $C_{52}H_{44}Cd_4N_{12}O_{12}$: C, 42.24; H, 3.00; N, 11.37%. Found: C, 42.69; H, 2.92; N, 11.55%. Selected IR data (KBr; cm^{-1}): 2174(vs), 1599(s), 1571(m), 1469(sh), 1434(s), 1384(s) 1312(s), 1263(m), 1228(m), 1113(m), 1052(s), 974(m), 958(m), 777(m), 753(m), 680(m), 634(m), 457(w), 435(w). UV–vis (solid state; λ_{max} [nm]): 308, 262 and 220. UV–vis (MeCN; λ_{max} [nm] (ε; $dm^3\ mol^{-1}\ cm^{-1}$)): 368 (59) and 269 (123 110).

Synthesis of $[Cd_4(NCO)_4\{(py)_2C(OH)(O)\}_2\{(py)_2C(OCH_3)(O)\}_2]$ (7). The synthetic procedure was similar to that of 2, except that the ammonium thiocyanate was replaced with sodium cyanate (0.085 g, 1.3 mmol). White crystals of 7 were obtained in 65% yield. Anal. calc. for $C_{50}H_{40}Cd_4N_{12}O_{12}$: C, 41.40; H, 2.78; N, 11.59%. Found: C, 41.75; H, 2.86; N, 11.36%. Selected IR data (KBr; cm^{-1}): 3449(br), 2170(vs, br), 1598(s), 1570(m), 1468(m) 1436(s), 1385(m), 1297(m), 1264(m), 1229(m), 1131(s), 1113(s), 1088(s), 1048(s), 1016(s), 956(m), 788(s), 752(s), 590(m), 457(m), 434(m). UV–vis (solid state; λ_{max} [nm]): 434, 359, 262 and 217. UV–vis (MeCN; λ_{max} [nm] (ε; $dm^3\ mol^{-1}\ cm^{-1}$)): 341 (307) and 262 (165 120).

Synthesis of $[Cd_4(N_3)_2(NO_3)_2\{(py)_2C(OH)(O)\}_2\{(py)_2C(OCH_3)(O)\}_2]$ (8). The synthetic procedure was similar to that of 3, except that ammonium thiocyanate was replaced with sodium azide (0.043 g, 0.65 mmol). White crystals of 8 were obtained in 70% yield. Anal. calc. for $C_{50}H_{40}Cd_4N_{12}O_{12}$: C, 37.07; H, 2.70; N, 15.04%. Found: C, 37.62; H, 2.82; N, 15.55%. Selected IR data (KBr; cm^{-1}): 3383(br), 2070(vs), 2033(sh), 1599(s), 1571(w), 1468(m), 1435(s), 1384(s), 1310(m), 1228(m), 1130(m), 1112(m), 1052(s), 1015(m), 974(w), 957(m), 788(m), 776(m), 752(m), 680(m), 635(m), 434(m). UV–vis (solid state; λ_{max} [nm]): 263 and 217. UV–vis (MeCN; λ_{max} [nm] (ε; $dm^3\ mol^{-1}\ cm^{-1}$)): 352 (537) and 269 (41 006).

Synthesis of $[Cd_4(NCO)_2(NO_3)_2\{(py)_2C(OH)(O)\}_2\{(py)_2C(OCH_3)(O)\}_2]$ (9a and 9b). The same synthetic procedure as that for 3 was used, except that ammonium thiocyanate was replaced with sodium cyanate (0.043 g, 0.65 mmol). The crystals of **9a** and **9b** have distinctive crystal forms: triangle and rhombic plates, respectively (Scheme 3). As the portion of **9a** was <5%, the mixture was not separated for further analyses and studies. Anal. calc. for $C_{48}H_{40}Cd_4N_{12}O_{16}$: C, 38.68; H, 2.70; N, 11.28%. Found: C, 38.33; H, 2.64; N, 11.52%. Selected IR data (KBr; cm^{-1}): 3453(m), 2173(vs), 1599(s), 1571(m), 1470(m), 1434(s) 1385(s), 1312(s), 1262(m), 1226(m), 1151(m), 1114(m), 1051(s), 1015(m), 974(m), 956(m), 778(m), 753(m), 670(m), 635(m), 434(w). UV–vis (solid state; λ_{max} [nm]): 311, 262 and 218. UV–vis (MeCN; λ_{max} [nm] (ε; dm^3 mol^{-1} cm^{-1})): 384 (149) and 274 (79 391).

Physical measurements

IR spectra were recorded on a Nicolet iS5 FT-IR spectrophotometer in the spectral range of 4000–400 cm^{-1} with the samples in the form of KBr pellets. Absorption UV–vis spectra were recorded on a UV–vis-NIR Nicolet iS50 double beam spectrophotometer. The steady-state and time-resolved emission spectra were measured for the solid state and MeCN solutions in ambient temperature on a FLS-980 fluorescence spectrophotometer equipped with a 450 W Xe lamp and a high-gain photomultiplier PMT+500nm (Hamamatsu, R928P) detector. The PL lifetime measurement was performed with a time correlated single photon counting (TCSPC) method. The excitation wavelength (340, 370 and 470 nm) was obtained using a TCSPC diode with a 100 ns pulse period as a light source and a PMT was used as a detector. IRF was designated using sample (solid state measurement) or a Ludox solution as a standard. The quantum yields of fluorescence were determined using an absolute method in room temperature, using an integrating sphere with the solvent as a blank.

X-ray powder diffraction (XRPD) measurements were performed on a PANalytical Empyrean X-ray diffractometer using Cu-Kα radiation (λ = 1.5418 Å) or Co-Kα radiation (λ = 1.789 Å), in which the X-ray tubes were operated at 40 kV and 30 mA ranging from 5 to 80°.

The DSC measurements were made with the DSC 200 F3 Maia differential scanning calorimeter (NETZSCH). The measurements were performed under a flow of analytical grade nitrogen (flow rate of 20.0 cm^3 min^{-1}) in the temperature range of 293.16–673.16 K. Aluminum crucibles were used with a mass difference smaller than 0.005 mg and a heating rate 20.0 K min^{-1} was applied. The specific heat capacity of all crucibles was tested before measurements and the difference between the reference crucible and the sample containing crucible was not larger than 0.01 J g^{-1}. The temperature and enthalpy were calibrated with usage of six spectrally pure standards: adamantane, In, Sn, Bi, Zn and CsCl. The sample mass was 3.02, 2.33, 1.53, 1.50, 3.00, 5.09, 1.96 and 3.25 mg for **1**, **2**, **4**, **5**, **6**, **7**, **8** and **9a** and **9b**, respectively.

Crystal structure determination and refinement

The X-ray intensity data of **1–9** were collected on an Gemini A Ultra Oxford Diffraction four-circle kappa geometry diffractometer with an Atlas CCD detector and graphite monochromatic MoKα radiation (λ = 0.71073 Å) at 293.0(2) K. The unit cell determination and data integration were carried out using the CrysAlis package of Oxford Diffraction.[10] Intensity data were corrected for the Lorentz and polarization effects. The absorption correction was introduced by SCALE3 ABSPACK scaling algorithm.[10] The structures were solved by the Patterson method using SHELXS-97 and refined by full matrix least-squares on F^2 with SHELXL-97 with anisotropic displacement parameters for non-hydrogen atoms.[11] Hydrogen atoms were placed in calculated positions refined using idealized geometries (riding model) and assigned fixed isotropic displacement parameters, d(C–H) = 0.93 Å, U_{iso}(H) = 1.2 U_{eq}(C) (for aromatic); and d(C–H) = 0.96 Å, U_{iso}(H) = 1.5 U_{eq}(C) (for methyl). The methyl groups were allowed to rotate about their local threefold axis. Details concerning crystal data and refinement are summarized in Tables S1 and S2.† The hydrogen bonds and selected bond distances and angles of **1–9** are listed in Tables S3–S12 (ESI†).

Results and discussion

Synthesis and general characterization

The compounds $[Cd(SCN)_2\{(py)_2C(OCH_3)(OH)\}]_n$ (**1**), $[Cd_2(SCN)_4\{(py)_2C(OCH_3)(OH)\}_2]$ (**2**), $[Cd_4(SCN)_4\{(py)_2C(OCH_3)(O)\}_4]$ (**3**), $[Cd_4(N_3)_4\{(py)_2C(OCH_3)(O)\}_4]$ (**4**), $[Cd_4(N_3)_4\{(py)_2C(OH)(O)\}_2\{(py)_2C(OCH_3)(O)\}_2]$ (**5**), $[Cd_4(NCO)_4\{(py)_2C(OCH_3)(O)\}_4]$ (**6**), $[Cd_4(NCO)_4\{(py)_2C(OH)(O)\}_2\{(py)_2C(OCH_3)(O)\}_2]$ (**7**), $[Cd_4(N_3)_2(NO_3)_2\{(py)_2C(OH)(O)\}_2\{(py)_2C(OCH_3)(O)\}_2]$ (**8**) and $[Cd_4(NCO)_2(NO_3)_2\{(py)_2C(OH)(O)\}_2\{(py)_2C(OCH_3)(O)\}_2]$ (**9a** and

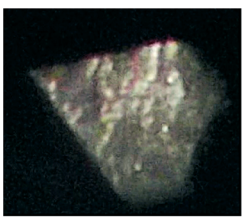

9a

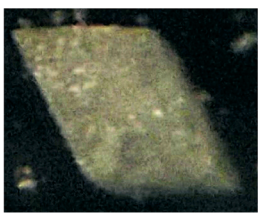

9b

Scheme 3 Crystal forms of **9a** and **9b**.

9b) have been synthesized *via* a self-assembly process by reacting NH_4SCN, NaN_3 or NaCNO with $Cd(NO_3)_2$ and the heterocyclic ligand di-2-pyridyl ketone [$(py)_2CO$]. In all the reactions the metal-to-organic ligand ratio was equal, 1 : 1. The synthetic strategy for **1**–**9** is presented in Scheme 4.

As it can be seen in Scheme 4, the pseudohalide ligand and reaction variables such as the molar ratio of metal precursor to pseudohalide anions and temperature strongly influence the structural versatility of the Cd(II)–$(py)_2CO$–X systems. The 1 : 1 : 2 reactions between $Cd(NO_3)_2{\cdot}4H_2O$, di-2-pyridyl ketone and NaN_3 or NaNCO in MeOH yielded tetranuclear compounds: $[Cd_4(X)_4\{(py)_2C(OCH_3)(O)\}_4]$ (X = N_3^- in **4** and NCO^- in **6**) – when the syntheses were carried out under reflux, and $[Cd_4(X)_4\{(py)_2C(OH)(O)\}_2\{(py)_2C(OCH_3)(O)\}_2]$ X = N_3^- in **5** and NCO^- in **7**) – at room temperature. In contrast, the 1 : 1 : 2 reactions of $Cd(NO_3)_2{\cdot}4H_2O$, $(py)_2CO$ and NH_4SCN resulted in the formation of one-dimensional coordination polymer $[Cd(SCN)_2\{(py)_2C(OCH_3)(OH)\}]_n$ (**1**) – under reflux, and $[Cd_2(SCN)_4\{(py)_2C(OCH_3)(OH)\}_2]$ (**2**) – at room temperature. A tetranuclear compound $[Cd_4(SCN)_4\{(py)_2C(OMe)(O)\}_4]$ was isolated by reacting $Cd(NO_3)_2{\cdot}4H_2O$, $(py)_2CO$ and NH_4SCN in a 1 : 1 : 1 molar ratio. Many attempts were made to obtain the tetranuclear compound of formula $[Cd_4(SCN)_4\{(py)_2C(OH)(O)\}_2\{(py)_2C(OCH_3)(O)\}_2]$, but all the efforts were in vain. The use of a 1 : 1 : 1 molar ratio of $Cd(NO_3)_2{\cdot}4H_2O$, $(py)_2CO$ and NaN_3 or NaNCO in MeOH at room temperature led to the formation of $[Cd_4(X)_2(NO_3)_2\{(py)_2C(OH)(O)\}_2\{(py)_2C(OCH_3)(O)\}_2]$. In all cases, the metal-promoted solvation of the ketocarbonyl group of $(py)_2CO$ occurs and the formation of the *gem*-diol form $(py)_2C(OH)_2$ or hemiketal form $(py)_2C(OCH_3)(OH)$ is observed. Depending on the type of pseudohalide ligand and reaction conditions, the *gem*-diol, hemiketal or their deprotonated forms (Scheme 4) coordinate to the metal center in a tridentate way *N*,*N*′,*O*.

The phase purity of the complexes was verified by PXRD measurements. As shown in Fig. S1–S8 (ESI†), the XRPD patterns measured for the polycrystalline samples were in good agreement with the XRPD patterns simulated from the respective single-crystal X-ray data using the Mercury 2.4 program,[12] demonstrating that the crystal structures are truly representative of the bulk materials.

In the high frequency region (3460–3100 cm^{-1}), the IR spectra of **1**, **2**, **5** and **7**–**9** show broad absorptions, assignable to O–H stretching vibrations. Intense absorptions associated with the stretching modes of SCN^- ions occur at 2117 and 2084 cm^{-1} for **1**, 2126 and 2100 cm^{-1} for **2**, and 2094 cm^{-1} for **3**. The occurrence of two strong absorptions for **1** and **2** is in agreement with the two different coordination modes of the thiocyanate groups in these structures. The stretching vibrations of N_3^- ions are seen as strong as very strong absorptions at 2048 cm^{-1} for **4**, 2064 and 2036 cm^{-1} for **5** and 2070 cm^{-1} for **8**, whereas the stretching modes ν_a(NCO) occur at 2174 cm^{-1} for **6**, 2170 cm^{-1} for **7**, and 2173 cm^{-1} for **9**. The conversion of the sp^2 hybridized C atom in free $(py)_2CO$ to sp^3 in $(py)_2C(OH)_2$, $(py)_2C(OR)(OH)$ and their deprotonated forms **1**–**9** is evidenced by the disappearance of the absorption band associated with the carbonyl group (at 1683 cm^{-1} for free $(py)_2CO$) and enhancement of the band at ~1040 cm^{-1} attributed to the stretching vibration of the C–O bond.[13] Finally, the spectrum of the mixture of **9a** and **9b** does not contain any obvious splitting and duplication of the bands, which proves that the oscillators of both compounds have a similar strength (Fig. S9–S16 in the ESI†).

The heating (under a nitrogen atmosphere) of the compounds containing the bridging $\mu_{1,3}$-SCN ions (**1** and **2**) or $\mu_{1,1}$-NCO ones (with the exception of **9**) leads to melting of the compounds, at about 400 K (**1** and **2**) and 480 K (**3**) directly followed by the decomposition (starting at about 430 K (**1** and **2**) and 510 K (**3**)). The melting of compounds **1** and **2** is a fast process exhibiting as the strong endothermic peak on the DSC curve (about 30 K wide), while the melting of compound **7** is a slow transformation (displayed by a broad endothermic peak with four overlapping, but distinguishable maxima). The similarity of the processes observed for the compounds **1** and **2** originates from the analogous linkage of the same anion (SCN^-) to the metal centres, and the dissimilarity of the effect observed for **7** (accompanied by higher thermal stability) is caused by the subsequent dissociation of

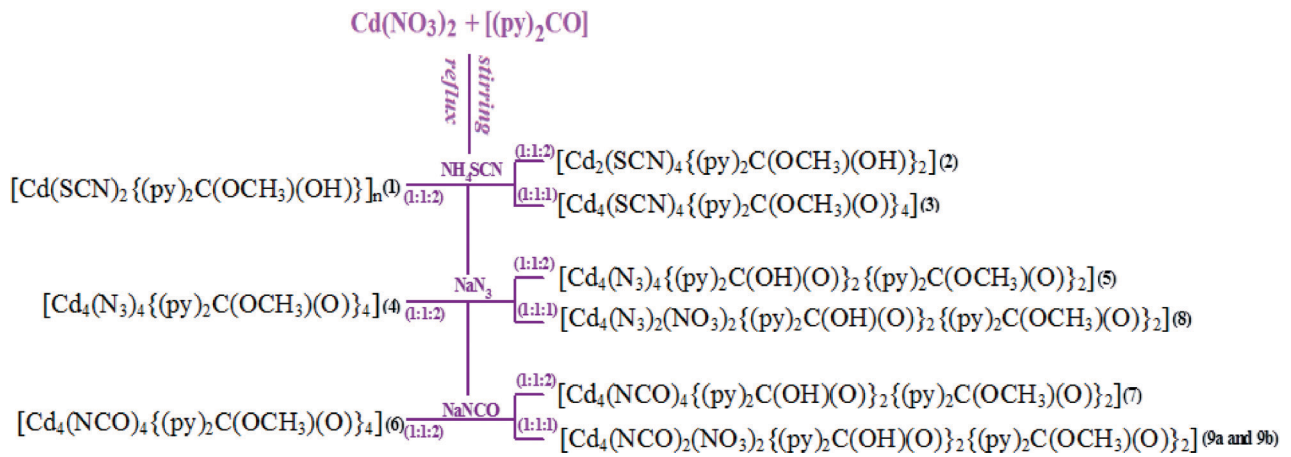

Scheme 4 The synthetic strategy for **1**–**9**.

the coordination bonds formed by the NCO ion (the $\mu_{1,1}$ coordination *versus* $\mu_{1,3}$ coordination). The final decomposition processes start above 550 K and lead to elemental carbon as a dominant solid product (confirmed by the XRPD diffraction of the sinter) in the cases of **1** and **2**. Compound **7** retains some of the initial composition, as it is observed during cooling of the samples (the exothermic crystallisation in the temperature range of 588–579 K, with an enthalpy of −9.2 J g^{-1}(residue)).

The heating of compounds possessing solely $\mu_{1,1}$-NCO or $\mu_{1,1}$-N_3 bridges or nitrate ions (**4–6**, **8** and **9**) leads in each case to a vigorous exothermic decomposition process (with an enthalpy larger than −280 kJ mol^{-1}) starting at almost 500 K, and preceded by a very small endothermic effect (with an enthalpy about 10 kJ mol^{-1}), associated with the formation of the quasi-liquid films on the sample surfaces. Further elevation of temperature leads to subsequent, overlapping stages of thermal decomposition of formed transition products. These processes lead to elemental carbon as a dominant solid product. The high thermal stability of these compounds (about 100 K larger than that of compounds **1**, **2**, and **7**) originates from the formation of the stable coordination core *via* bridging atoms. The observed difference in thermal stability and behaviour between **7** and **9** may be attributed to the presence of the chelating NO_3^- ions (the chelation in **9** increases the stability in comparison to the terminal binding of two monodentate NCO^- ions of **7**, and the oxidative properties of NO_3^- ions favour decomposition over melting). The DSC analysis of the compounds **9a** and **9b** does not show the presence of the two different polymorphs of the compounds (the first extremum exhibits the regular sharp shape), even in the case of the study of the evident mixture of both polymorphs (determined *via* the XRPD). This effect originates from the character of the first process. Typically the polymorphic forms differ in the crystal lattice energy as a result of the different characters of intermolecular interactions in the crystal net. Consequently the polymorphs possess different enthalpies of fusion. Compound **9** decomposes without melting, which means that the energetic effects are molecular-structure related, and they are not governed by the crystal structure. Regardless of the process character (melting or decomposition), **9a** and **9b** do not form any strong or medium strength hydrogen bonds, thus the energetic effects related to the degradation of the crystal net are negligible (see also Fig. S17–S24†).

Structure of $[Cd(NCS)_2\{(py)_2C(OCH_3)(OH)\}]_n$ (1)

Compound **1** crystallizes in the chiral orthorhombic space group $P2_12_12_1$. Single-crystal X-ray diffraction analysis was performed for eight crystals, randomly picked from the same reaction. The Flack parameters of the eight crystals were all close to zero (Tables S1 and S2†), indicating a large degree of enantiomeric purity within the crystal.[14] Furthermore, the results demonstrated that the bulk material contained only single crystals of M helices.

The X-ray crystal structure analysis revealed that the cadmium(II) centres in **1** are singly bridged by end-to-end thiocyanate ions with the formation of an infinite left-handed helical chain, coincident with the 2_1 screw axes along the *a* crystal direction and with a pitch of 8.9163(4) Å which is equal to the *b* axis length (Fig. 1). The intrachain Cd···Cd separation of 6.181(4) Å is in accordance with the values reported for related cadmium(II) structures based on single thiocyanate bridges, 6.006 Å in $[Cd_3(tren)_2(SCN)_6]_n$,[15] 6.232 Å in $[Cd(ben)(SCN)_2]$ (ben is bis(2-aminoethyl)amine)[16] and 6.200 Å in $[Cd_3(NCS)_6(medien)_2]_n{\cdot}nH_2O$ (medien is *N*,*N*-bis(2-aminoethyl)methylamine).[17]

Each cadmium(II) centre is in a distorted $\{N_4OS\}$ octahedral coordination environment defined by two nitrogen and one oxygen atoms from the hemiketal form $(py)_2C(OCH_3)(OH)$, terminal N-coordinated thiocyanate anion and two $\mu_{1,3}$-SCN^- ions, one bounded by N and one by the S donor. The tridentate *N*,*N*′,O(CH_3) coordination mode produces a six-membered metallocyclic ring (Cd(1)–N(1)–C(5)–C(6)–C(7)–N(2)) and two five-membered (Cd(1)–N(1)–C(5)–C(6)–O(1) and Cd(1)–N(2)–C(7)–C(6)–O(1)) metallocyclic rings fused along the Cd(1)–O(1)–C(6). The pyridyl rings of the $(py)_2C(OCH3)(OH)$ ligand are planar and form a dihedral angle of 67.76(15)°. The two five-membered chelating rings Cd(1)–N(1)–C(5)–C(6)–O(1) and Cd(1)–N(2)–C(7)–C(6)–O(1) exist in the envelope form where the O(1) atom is 0.986(5) and 1.022(4) Å out of the plane of the remaining four atoms, respectively. The six-membered metallocyclic ring (Cd(1)–N(1)–C(5)–C(6)–C(7)–N(2)) is in a boat conformation with the Cd(1) and C(6) atoms being 0.964(6) and 0.791(6) Å, respectively, out of the best mean plane defined by the N(1), N(2), C(5) and C(7) atoms. The pyridyl nitrogens can be viewed as strongly coordinating to the metal (2.322(3) and 2.402(3) Å), while the methylated oxygen forms a weak bond to Cd(II) (2.603(3) Å).

The bridging and terminal thiocyanate units are quasi-linear as reflected in their bond angles of 177.3(4) and 179.0(5)°, respectively. Substantial bending occurs at the sulphur atom of the thiocyanate ion [C(99)^i–S(99)–Cd(1) = 101.84(16)°; i: $x - 1/2, -y + 1/2, -z + 1$].

The helical chains are assembled into a three-dimensional supramolecular framework (Fig. 1c) by a weak O(2)···S(99)^i interaction [(i): $2 - x$, $0.5 + y$, $1.5 - z$] with a distance of 3.228 Å, which is only marginally shorter than the sum of the van der Waals radii (3.3 Å).[18]

Structure of $[Cd_2(SCN)_4\{(py)_2C(OCH_3)(OH)\}_2]$ (2)

The structure of **2** consists of the dinuclear $[Cd_2(SCN)_4\{(py)_2C(OCH_3)(OH)\}_2]$ units as presented in Fig. 2a. The dimer results from the pairing of the two mononuclear units $[Cd(SCN)_2\{(py)_2C(OCH_3)(OH)\}]$, related by a crystallographic center of inversion. The Cd(II) ions are doubly bridged by thiocyanate anions in an end-to-end coordination mode. The double NCS^- bridge forms an essentially planar, rectangular eight-membered Cd($\mu_{1,3}$-SCN)$_2$Cd ring with an

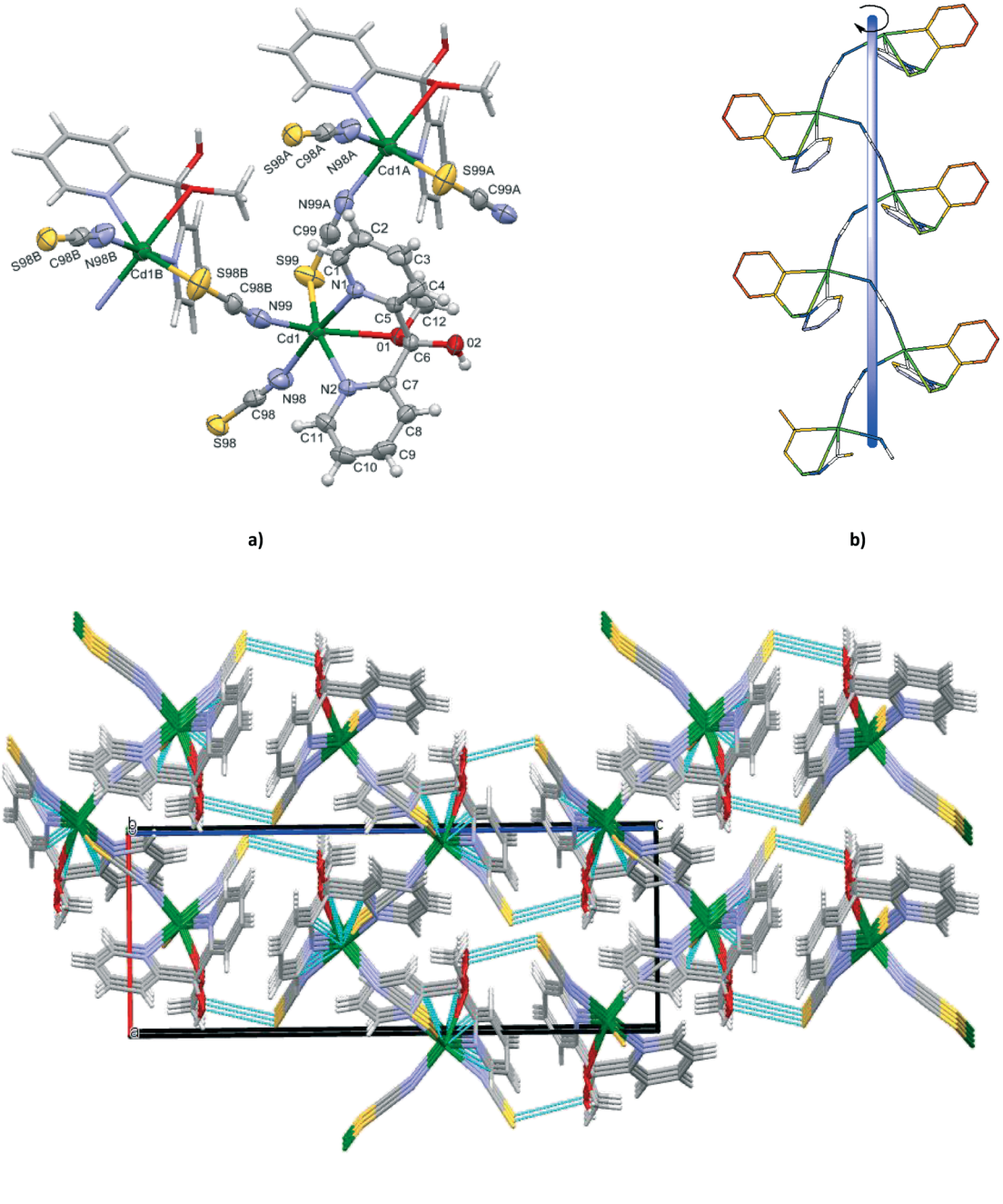

Fig. 1 (a) Perspective view of the fragment of $[Cd(SCN)_2\{(py)_2C(OCH_3)(OH)\}]_n$ (**1**) showing the atom numbering. Displacement ellipsoids are drawn at 50% probability. Symmetry codes: (A) = $x + 1/2, -y + 1/2, -z + 1$, (B) = $x - 1/2, -y + 1/2, -z + 1$; (b) perspective view of M helix; (c) view of the three dimensional supramolecular network formed *via* a weak interaction O(2)···S(99)^{i} [(i): $2 - x, 0.5 + y, 1.5 - z$) interactions shown by dotted lines.

intradinuclear Cd···Cd separation of 5.4826(6)Å, slightly shorter in comparison with the related dinuclear cadmium(II) coordination compounds based on a double thiocyanate bridge and incorporating tridentate terminal co-ligand: 5.889 Å in $[Cd_2(C_{11}H_{14}N_3O_3)_2(\mu_{1,3}\text{-}SCN)_2(CH_4O)_2]$,[19] 5.659 Å in $[Cd_2(pydim)_2(\mu_{1,3}\text{-}SCN)]_2[BF_4]_2$,[20] 5.791 Å in $[Cd(L^1)(NCS)(\mu_{1,3}\text{-}SCN)]_2$ (L^1 = *N*-(4,6-dimethyl-pyrimidin-2-yl)-*N*′-pyridin-2-ylmethylene-hydrazine),[21] and 5.887 Å in $[Cd(L^2)(NCS)(\mu_{1,3}\text{-}SCN)]_2$ (L^2 = *N*,*N*-diethyl-*N*′-(1-pyridine-2-yl-ethylidene)-ethane-1,2-diamine).[22]

Each cadmium(II) ion is six-coordinated in a highly distorted $\{N_3S_2O\}$ octahedral geometry defined by two nitrogen and one oxygen atoms of the tridentate chelating $(2\text{-py})_2C(OCH_3)(OH)$ molecule, sulphur and nitrogen atoms from the bridging thiocyanate ligands and a sulphur atom from the terminally bound thiocyanate ion. The significant distortion from an ideal octahedron can be attributed to the *N*,*N*′,*O*-tridentate coordination of $(py)_2C(OCH_3)(OH)$ which elongated the M–O bond length (2.498(3) Å) as well as the

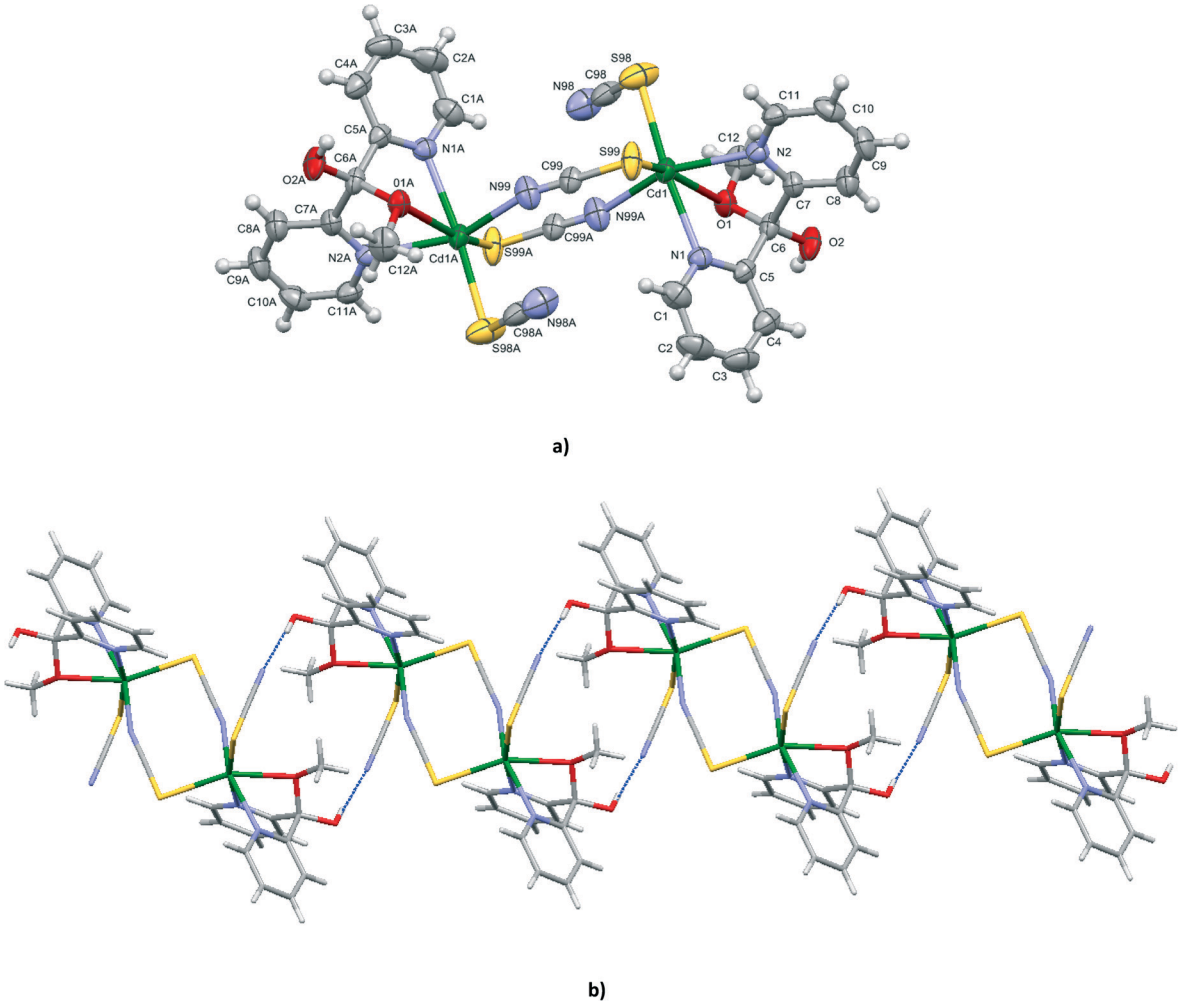

Fig. 2 (a) Molecular structure of $[Cd_2(SCN)_4\{(py)_2C(OCH_3)(OH)\}_2]$ (**2**) showing the atom numbering. Displacement ellipsoids are drawn at 50% probability. Symmetry codes: (A) = $-x, -y + 1, -z + 1$; (b) view of the packing of **2** showing the hydrogen bonds O(2)–H(2A)···N(98)^{i} [D···A distance = 2.769(7) Å and D–H···A angle = 167.0°; (i): $-x, 2 - y, 1 - z$].

length of the Cd–S distances (2.6336(14) and 2.5953(15) Å). Likewise in **2**, the six-membered chelate ring Cd(1)–N(1)–C(5)–C(6)–C(7)–N(2) adopts a boat conformation with the Cd(1) and C(6) atoms on the same side of the plane formed by the other four atoms. The dihedral angle between the mean planes of the two coordinated pyridyl rings is 68.86(18)°, very close to the value found in **1**. The bridging and terminal thiocyanate units are quasi-linear, as reflected in their bond angles of 178.4(4) and 177.9(6)°, respectively. Substantial bending occurs at the sulphur atom of the thiocyanate ions [C(98)–S(98)–Cd(1) = 99.45(18)° and C(99)–S(99)–Cd(1) = 92.58(17)°] and also at the nitrogen atom of the thiocyanate bridge [C(99)–N(99)–Cd(1)^{i} = 159.9(4)°; i: $-x, -y + 1, -z + 1$].

The neighbouring molecules $[Cd_2(SCN)_4\{(py)_2C(OCH_3)(OH)\}$ are linked through the O(2)–H(2 A)···N(98)^{i} hydrogen bonds involving the uncoordinated hydroxy oxygen of the $(py)_2C(OCH_3)(OH)$ and the nitrogen atom of the terminal thiocyanate ligand [D···A distance = 2.769(7) Å and D–H···A angle = 167.0°; (i): $-x, 2 - y, 1 - z$] into a 1D supermolecular chain network (Fig. 2b).

Structures of $[Cd_4(N_3)_4\{(py)_2C(OCH_3)(O)\}_4]$ (4) and $[Cd_4(NCO)_4\{(py)_2C(OCH_3)(O)\}_4]$ (6)

The compounds **4** and **6** crystallize in the tetragonal space group $I4_1/acd$ and their crystal structures consist of tetranuclear molecules $[Cd_4(N_3)_4\{(py)_2C(OCH_3)(O)\}_4]$ (in **4**) and $[Cd_4(N_3)_4\{(py)_2C(OCH_3)(O)\}_4]$ (in **6**) with cubane-like $[Cd_4(\mu_3\text{-}O)_4]^{4+}$ cores. The vertices of the cubane structures are alternately occupied by four Cd atoms and four oxygen atoms of monoanion $(py)_2C(OCH_3)O^-$, symmetrically related by a crystallographic four-fold inversion axis symmetry (Fig. 3). In addition to three μ_3 oxygen atoms, each Cd(II) center is coordinated to two N pyridine donors belonging to two different $(py)_2C(OCH_3)O^-$ ligands and one terminal pseudohalide ion (N_3^- in **4** and NCO^- in **6**) to complete an octahedral coordination environment. Each monoanion $(py)_2C(OCH_3)O^-$

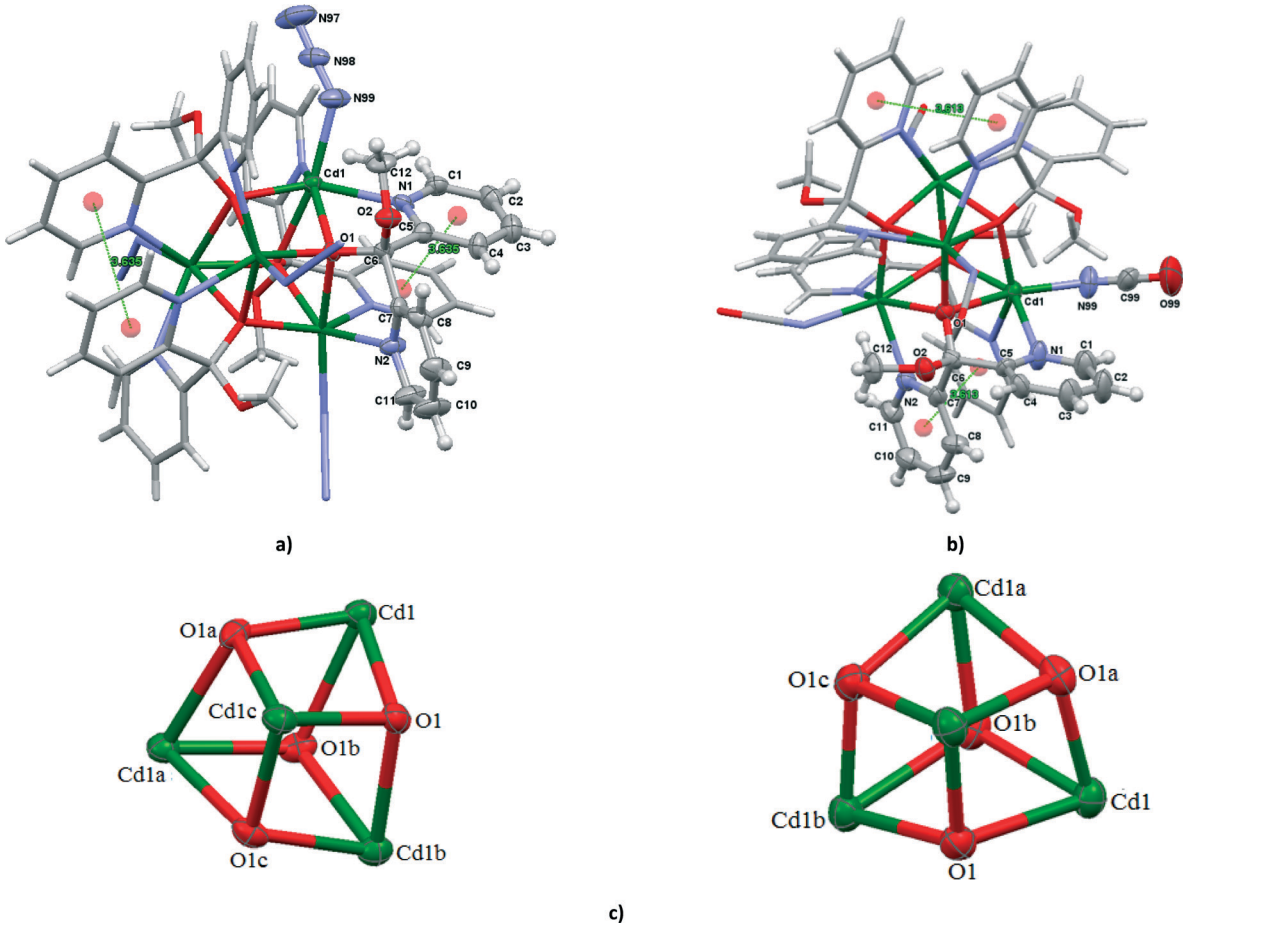

Fig. 3 Molecular structures of $[Cd_4(N_3)_4\{(py)_2C(OCH_3)(O)\}_4]$ (a) and $[Cd_4(NCO)_4\{(py)_2C(OCH_3)(O)\}_4]$ (b). Displacement ellipsoids are drawn at 50% probability; (c) cubane unit schemes of $[Cd_4(\mu_3\text{-}O)_4]^{4+}$ core in $[Cd_4(N_3)_4\{(py)_2C(OCH_3)(O)\}_4]$ (symmetry code (a) = −3/4 − *y*, −1/4 + *x*, 1/4 − *z*; (b) = −1 − *x*, 1/2 − *y*, *z*, (c) = 1/4 + *y*, 3/4 − *x*, 1/4 − *z*) and $[Cd_4(NCO)_4\{(py)_2C(OCH_3)(O)\}_4]$ (symmetry code (a) 3/4 − *y*, −1/4 + *x*, 5/4 − *z*; (b) = 1 − *x*, 1/2 − *y*, *z*, −*z* + 5/4; (c) = 1/4 + *y*, 3/4 − *x*, 5/4 − *z*).

coordinates to three Cd(II) centers forming two five-membered chelating rings with two different metals and an alkoxide type bond to a third Cd(II) atom. The dihedral angle between the mean planes of the pyridyl rings belonging to the same $(py)_2C(OCH_3)O^-$ ligand is 79.87° in **4** and 81.18° in **6**. Upon coordination, the monoanion $(py)_2C(OCH_3)O^-$ forms one short (2.246(4) Å in **4** and 2.248(5) Å in **6**) and two elongated (2.392(3) and 2.449(4) Å in **4**, 2.363(5) and 2.248(5) Å in **6**) Cd–O bond lengths. The different Cd–O bond lengths are reflected in the Cd⋯Cd separations; the face diagonal vectors Cd⋯Cd are 3.6502(8) and 3.6617(8) Å in **4** and 3.6515(8) and 3.6603(8) Å in **6**. The cube clearly deviates from the ideal geometry. The internal cube angles at the metal vertices have values 79.37(13) 76.33(14) and 75.17(13)° in **4** and 79.50(18) 75.11(18) and 77.52(19)° in **6**, whereas the comparable angles at the alkoxide corners are larger than 90°, 97.90(13), 102.49(14) and 104.31(14)° in 4 and 98.12(17), 100.98(19) and 104.69(19)° in **6**. The pyridyl rings are involved in π–π interactions; 3.636(3) Å for Cg(23)^{i}((N(1)–C(1)–C(5))⋯Cg(23)((N(1)–C(1)–C(5)) centroids for **4** and 3.613(5) Å for Cg(24)^{i}((N(2)–C(7)–C(11))⋯Cg(23)((N(2)–C(7)–C(11)) centroids for **6** (i) = 1 − *x*, 1/2 − *y*, *z*.

Structures of $[Cd_4(N_3)_4\{(py)_2C(OH)(O)\}_2\{(py)_2C(OCH_3)(O)\}_2]$ (5) and $[Cd_4(NCO)_4\{(py)_2C(OH)(O)\}_2\{(py)_2C(OCH_3)(O)\}_2]$ (7)

The structures of **5** and **7** consist of the centrosymmetric tetranuclear (binuclear of binuclear) cadmium(II) compounds $[Cd_4(N_3)_4\{(py)_2C(OH)(O)\}_2\{(py)_2C(OCH_3)(O)\}_2]$ (**5**) and $[Cd_4(NCO)_4\{(py)_2C(OH)(O)\}_2\{(py)_2C(OCH_3)(O)\}_2]$ (**7**) showing double open cubane-like structures with two missing vertices (Fig. 4). The dicubane-like cores in **5** and **7** are stabilized by hydrogen bond O(4)–H(4A)⋯O(1)^{i} [D⋯A distance = 2.717(3) Å and D–H⋯A angle = 171.0°; (i): −*x*, 1 − *y*, 1 − *z* in **5** and D⋯A distance = 2.738(7) Å and D–H⋯A angle = 171.0°; (i): 1 − *x*, 1 − *y*, −*z* in **7**].

The crystallographically related Cd(1) and Cd(1a) atoms are doubly bridged through the deprotonated oxygen atoms O(3) and O(3a) of the monoanion $(py)_2C(OH)O^-$. The atoms O(3) and O(3a) occupy two other vertices and act as triple bridges also bound to the Cd(2) and Cd(2a) atoms, respectively. In addition, the Cd(1) atoms are bridged to the Cd(2) through the deprotonated oxygen atom O(1) of the monoanion $(py)_2C(OCH_3)O^-$, and to Cd(2a) through the nitrogen atom N(99) of the end-to-on N_3^- ion in **5** or end-to-on NCO^-

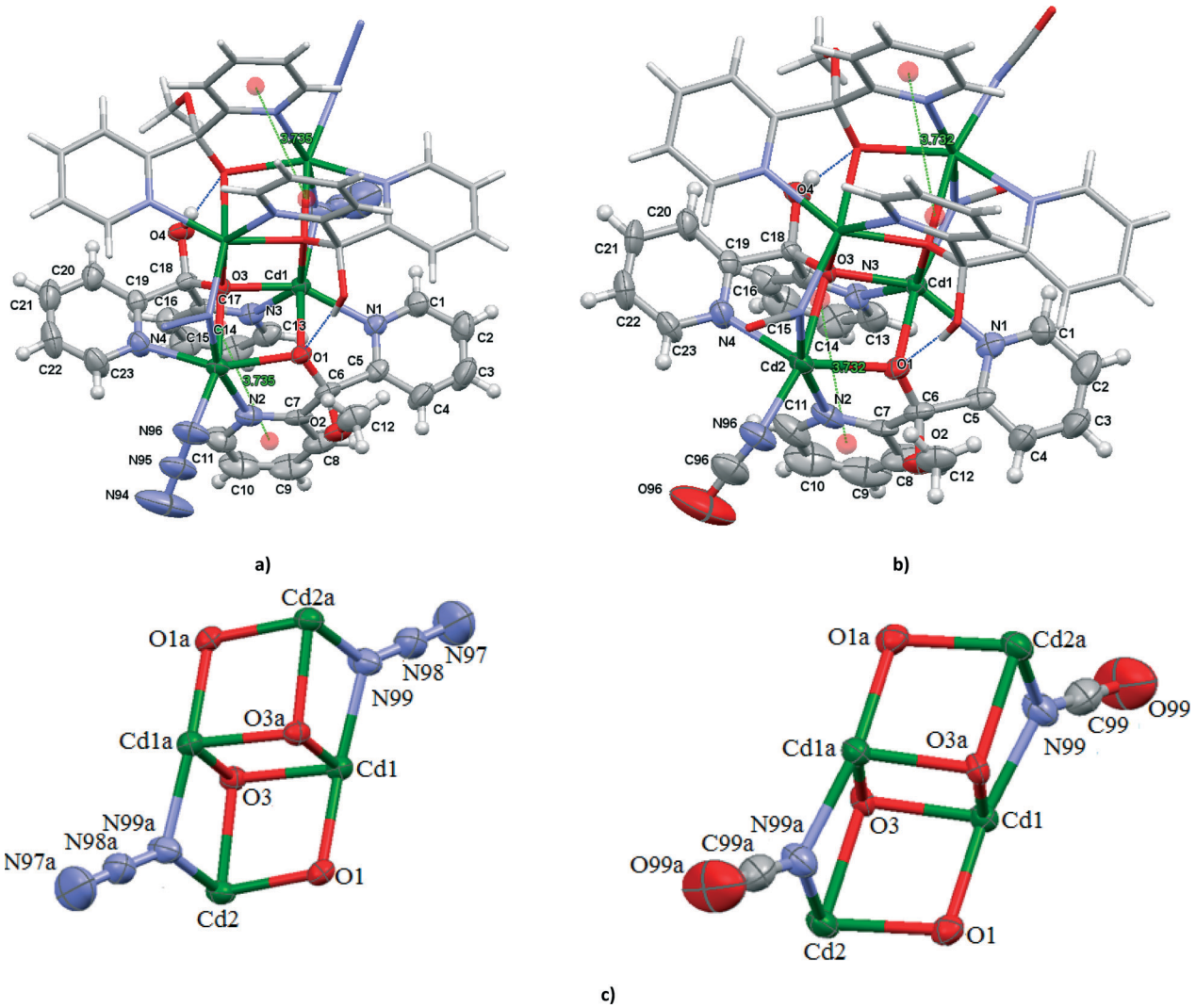

Fig. 4 Molecular structures of $[Cd_4(N_3)_4\{(py)_2C(OH)(O)\}_2\{(py)_2C(OCH_3)(O)\}_2]$ (a) and $[Cd_4(NCO)_4\{(py)_2C(OH)(O)\}_2\{(py)_2C(OCH_3)(O)\}_2]$ (b). Displacement ellipsoids are drawn at 50% probability; (e) dicubane unit schemes in $[Cd_4(N_3)_4\{(py)_2C(OH)(O)\}_2\{(py)_2C(OCH_3)(O)\}_2]$ (symmetry code (a) = $-x$, $1-y$, $1-z$) and $[Cd_4(NCO)_4\{(py)_2C(OH)(O)\}_2\{(py)_2C(OCH_3)(O)\}_2]$ (symmetry code (a) = $1-x$, $1-y$, $-z$).

in **7**. The monoanions $(py)_2C(OH)O^-$ and $(py)_2C(OCH_3)O^-$ coordinate to the metal centers in an asymmetric way. The local environment around the Cd centers can best be described as a highly distorted octahedron. The Cd(1) atom is coordinated to two μ_3-oxygen atoms of the monoanions $(py)_2C(OH)O^-$, one μ_2-oxygen of $(py)_2C(OCH_3)O^-$, two pyridine nitrogen atoms and nitrogen donor of $\mu_{1,1}$-N_3^- (in **5**) or $\mu_{1,1}$-NCO^- (in **7**) bridge. The coordination sphere of the Cd(2) atom is composed of the μ_3-oxygen atom of the monoanion $(py)_2C(OH)O^-$, μ_2-oxygen atom of $(py)_2C(OCH_3)O^-$, two pyridine nitrogen atoms and two nitrogen donors of the terminal and bridging ions, N_3^- in **5** and NCO^- in **7**. The angles Cd–N_{azide}–Cd (101.37(13)°) and Cd–N_{NCO}–Cd (100.0(3)°) are similar to those reported in the literature for $[Cd_4(dafone)_4Cl_2(\mu_{1,1}\text{-}N_3)_4(\mu_{1,1,1}\text{-}N_3)_2]$ (93.49(18), 107.3(2) and 107.8(2)°)[23] and $[Cd(tp)(NCO)2]n$ (99.33(9) and 87.14(8)°).[24] The pyridyl rings are involved in π–π interactions; 3.735(3) Å for $Cg(18)^{ii}$((N(2)–C(7)–C(11))···Cg(19)((N(3)–C(13)–C(17)) centroids for **5** and 3.732(6) Å for $Cg(18)^{ii}$((N(2)–C(7)–C(11))···Cg(19)((N(3)–C(13)–C(17)) centroids for **6** (ii) = x, y, z].

Structures of $[Cd_4(N_3)_2(NO_3)_2\{(py)_2C(OH)(O)\}_2\{(py)_2C(OCH_3)(O)\}_2]$ (8) and $[Cd_4(NCO)_2(NO_3)_2\{(py)_2C(OH)(O)\}_2\{(py)_2C(OCH_3)(O)\}_2]$ (9a and 9b)

Like **1** and **7**, **8**, **9a** and **9b** are centrosymmetric tetranuclear (binuclear of binuclear) double open cubane-like compounds. In contrast to **1** and **7**, however, they possess two nitrate groups instead of terminal azide ions (Fig. 5). Interestingly, the compound $[Cd_4\{(py)_2C(OH)(O)\}_2\{(py)_2C(OCH_3)(O)\}_2(NCO)_2(NO_3)_2]$ was isolated in two polymorphic forms, monoclinic (**9a**), isostructural to **8**, and orthorhombic (**9b**).

The Cd(1) atom of **8** and **9** is coordinated to two μ_3-oxygen atoms of the monoanions $(py)_2C(OH)O^-$, one μ_2-oxygen of $(py)_2C(OCH_3)O^-$, two pyridine nitrogen atoms and nitrogen

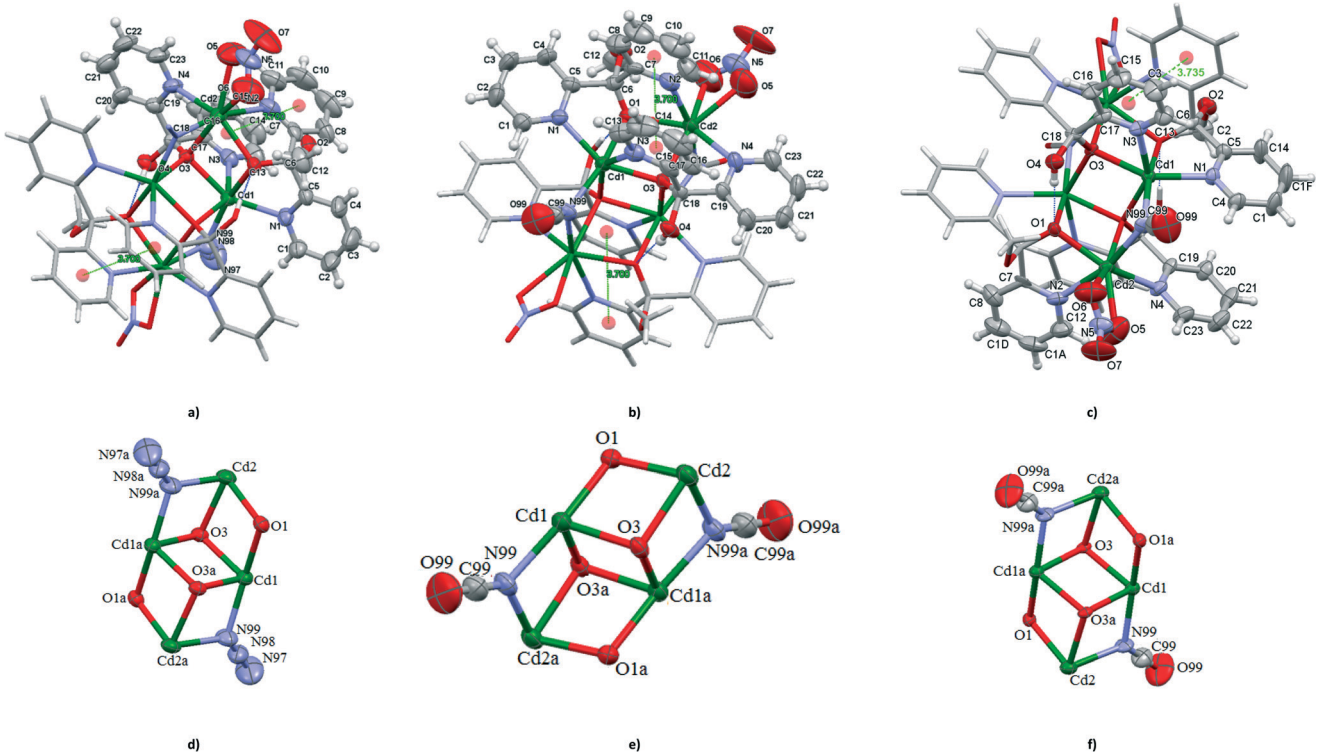

Fig. 5 Molecular structures of $[Cd_4(N_3)_2(NO_3)_2\{(py)_2C(OH)(O)\}_2\{(py)_2C(OCH_3)(O)\}_2]$ (a) and $[Cd_4(NCO)_2(NO_3)_2\{(py)_2C(OH)(O)\}_2\{(py)_2C(OCH_3)(O)\}_2]$ (b and c). Displacement ellipsoids are drawn at 50% probability; dicubane unit schemes in **8** (d; symmetry code (a) = 1 − *x*, −*y*, 1 − *z*), in **9a** (e; symmetry code (a) = −*x*, 1 − *y*, 1 − *z*) and **9b** (f; symmetry code (a) = 1 − *x*, 1 − *y*, 1 − *z*).

donor of $\mu_{1,1}$-N_3^- (in **5**) or $\mu_{1,1}$-NCO^- (in **7**) bridge. The coordination environments of Cd(2) is formed by two N pyridine donors belonging to $(py)_2C(OCH_3)O^-$ and $(py)_2C(OCH_3)O^-$ ligands, nitrogen atom of the bridging pseudohalide ion (N_3^- in **8** and NCO^- in **9**), μ_3-oxygen atom of the monoanion $(py)_2C(OH)O^-$, μ_2-oxygen of $(py)_2C(OCH_3)O^-$ and two oxygen atoms of the nitrate group acting as chelating bidentate ligand. The geometrical distortion of the Cd(2) ions in **8** and **9** from ideal possible seven-vertex polyhedra (pentagonal bipyramid (PBPY), capped octahedron (COC) and capped trigonal prism (CTP)) have been calculated using the SHAPE program[25] based on the Continuous Shape Measures (CShM) concept. Mathematically, the CShM of the original structure (Q) is a normalized root-mean-square deviation of the referenced structure with the desired symmetry (P) and it is expressed by eqn (1):

$$S_Q(P) = \min\left[\frac{\sum_{i=1}^{n} |\vec{q}_i - \vec{p}_i|^2}{\sum_{i=1}^{n} |\vec{q}_i - \vec{q}_0|^2}\right] \times 100 \qquad (1)$$

where q_i represents the N vectors that contain the $3N$ Cartesian coordinates of the problem structure Q, and p_i contains the coordinates of the ideal polyhedron P and q_0 is the position vector of the geometric center that is chosen to be the same for the two polyhedra.[26]

The calculated distances to the capped octahedron (5.043 for **8**, 5.201 for **9a** and 5.092 for **9b**), capped trigonal prism (4.581 for **8**, 4.904 for **9a** and 4.211 for **9b**) and PBPY (4.047 for **8**, 3.995 for **9a** and 4.074 for **9b**) indicate severe distortions of the geometry of the Cd(2) ions in **8**, **9a** and **9b** from all ideal seven-vertex polyhedra.

The bond lengths between the cadmium and oxygen atoms of the nitrate (2.427(5) and 2.491(6) Å in **8**, 2.435(6) and 2.491(6) Å in **9a** and 2.435(8) and 2.500(7) Å in **9b**) are similar to the average value of 2.454(8) Å calculated for 55 coordination compounds incorporating the bidentate nitrate group and tridentate N-donor ligand; the mean value of the bond distance between the cadmium atom and the oxygen atom of the monodentate nitrate group calculated for 40 coordination compounds containing tridentate N-donor ligand is 2.401(1) Å.[6] The bidentate fashion of nitrate ion in **8**, **9a** and **9b** is also evidenced by the criteria introduced by Kleywegt, *et al.* (see Scheme 5).[27]

Similar to **1** and **7**, the dicubane-like core of **8** and **9** is stabilized by hydrogen bond O(4)–H(4A)···O(1)^{i} [D···A distance = 2.712(4) Å and D–H···A angle = 177.0°; (i): 1 − *x*, −*y*, 1 − *z* in **8** and D···A distance = 2.707(7) Å and D–H···A angle = 171.0°; (i): −*x*, 1 − *y*, 1 − *z* in **9a** and D···A distance = 2.705(6) Å and D–H···A angle = 177.0° in **9b**]. Also, the structural parameters of the double open cubane-moiety of **8** and **9** correlate well with the values for **1** and **7**.

The pyridyl rings are involved in π–π interactions; 3.700(4) Å for Cg(5)^{ii}((N(2)–C(7)–C(11))···Cg(6)((N(3)–C(13)–C(17))

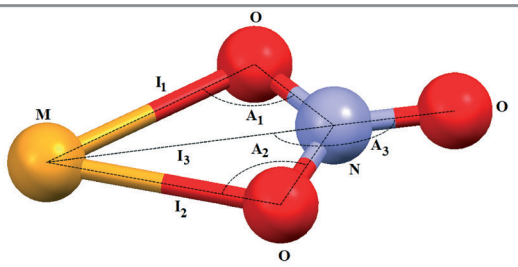

	Monodentate	Anisobidentate	Bidentate	8	9a	9b
$I_2–I_1$ (Å)	>0.6	0.3–0.6	<0.3	0.064	0.056	0.065
$A_1–A_2$ (°)	>28	14–28	<14	3.4	3.3	3.6
$I_3–I_2$	<0.1	0.1–0.2	>0.2	0.423	0.438	0.409
A_3 (°)	<162	162–168	>168	177.43	174.94	178.49

Scheme 5 Parameters used for determining nitrate coordination mode[27] and appropriate values for coordinated nitrate group in **8**, **9a** and **9b**.

centroids for **8** and 3.700(5) Å for Cg(5)^{ii}((N(2)–C(7)–C(11))···Cg(6)((N(3)–C(13)–C(17)) centroids for **9a**, and 3.735(5) Å for Cg(6)^{iii}((N(2)–C(7)–C(8)–C(10)–C(1a)–C(12))···Cg(7)((N(3)–C(13)–C(3)–C(15)–C(16)–C(17)) centroids for **9b**, and (ii) = x, y, z; (iii) = 1 − x, 1 − y, 1 − z.

Luminescence properties

The excitation and emission spectra of the Cd(II) compounds and free $(py)_2CO$ were recorded in MeCN solution and in the solid state at room temperature. A summary of the photophysical data is provided in Table 1. The normalized emission spectra of **1**, **2**, **4–9** and free $(py)_2CO$ in MeCN and the solid state are shown in Fig. 6 and 7, respectively. The nanosecond range of lifetime in MeCN solution and the solid state suggests the fluorescent nature of the emissions (Table 1).

Irradiation of **2** and **4–9** in solution with wavelengths of 328–365 nm gave rise to a structureless emission band with maxima in the ranges of 446–460 nm and Stokes shifts of 5125–8763 cm^{-1}, respectively. Compared to the free ligand (λ_{ex} = 300 nm, λ_{ex} = 407 nm), the emission and excitation wavelengths of the coordination compounds are red-shifted (Table 1 and Fig. 6).

Taking into consideration that Cd(II) ions are difficult to oxidize or reduce due to their d^{10} configuration, however, it can be assumed that the emissions of **2** and **4–9** are neither metal-to-ligand charge transfer (MLCT) nor ligand-to-metal charge transfer (LMCT) in nature. It is highly probable that the emitting excited state of the Cd(II) compounds has an IL (intraligand) character. The red shift of the emission maximum with respect to the free ligand may be due to the following reasons: (i) the organic ligand may change their highest occupied molecular orbital (HOMO) and lowest

Table 1 Summary of photoluminescence properties of $(py)_2CO$ and cadmium coordination compounds

Compound	Medium	λ_{ex} [nm]	λ_{em} [nm]	Stokes shifts [cm^{-1}]	τ, ns, (%)	χ^2
$(py)_2CO$	Solid	Non-emissive				
	MeCN	300	407	8763	1.62 (65.51%), 3.19 (34.49%)	0.988
1	Solid	437	509	3237	1.75 (39.07%), 6.47 (60.93%)	1.024
	MeCN	—	—	—	—	—
2	Solid	Non-emissive				
	MeCN	328	453	8413	2.55	1.134
4	Solid	368	438	4343	0.88 (52.10%), 4.37 (47.90%)	1.012
	MeCN	365	449	5125	2.00 (63.11%), 6.09 (36.99%)	1.223
5	Solid	365	436	4461	0.69 (52.8%), 3.74 (47.2%)	0.913
	MeCN	345	460	7247	2.91	1.049
6	Solid	351	427	5071	1.03 (60, 33%), 6.01 (39.67%)	1.180
	MeCN	339	457	7617	2.95 (100%)	0983
7	Solid	351	420/536	4680	0.79 (38.31%), 2.76 (33.19%), 6.55 (28.5%)	1.194
	MeCN	345	458	7152	2.94	1.011
8	Solid	351	411	4159	0.66 (71.65%), 3.79 (28.37%)	1.174
	MeCN	342	457	7358	2.91	1.043
9a and **9b**	Solid	360	440	5051	0.64 (80.77%)	1.021
	MeCN	335	446	7429	2.95 (80.77%)	0.983

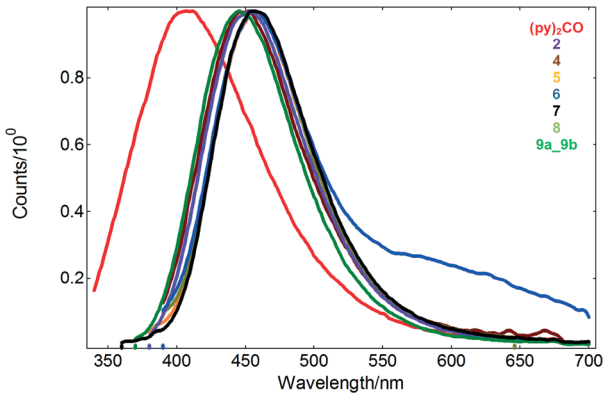

Fig. 6 The emission spectra of the free ligand and Cd(II) compounds in acetonitrile solution (10^{-4} M).

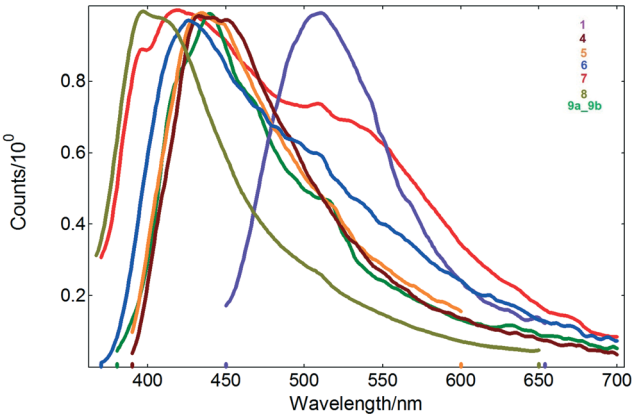

Fig. 7 The solid state emission spectra of Cd(II) coordination compounds.

unoccupied molecular orbital (LUMO) energy levels after coordination to metal centers; (ii) ligand to ligand charge transfer transitions may occur; and (iii) weak interactions may affect the energy transfer involved in the luminescence.

Except for **2**, the reported Cd(II) compounds show also luminescence in the solid state, with emission maxima in the range of 411–536 nm and nanosecond lifetimes (Table 1 and Fig. 7). Noteworthy, di-2-pyridyl ketone is non-emissive in the solid state. For compound **7**, the bimodal emission with maxima at 420 and 536 nm is observed, whereas excitation of the samples of **1**, **4**, **5**, **6**, **8** and **9** produces luminescence with one main peak at 509, 438, 436, 427, 411 and 440 nm, respectively.

Compared to the values reported for solution, the emission bands of **4**, **5**, **6**, **8** and **9** appear blue-shifted, consistent with the rigidochromic effect. Furthermore, there is a marked difference in the fluorescence maximum wavelength of the helical structure of **1** with respect to that recorded for the tetranuclear compounds **4**, **5**, **6**, **8** and **9** (Table 1). This effect is probably attributed to different coordination environments of the metal ions and conformational ligands as well as weak interactions in the network lattice which may affect the rigidity of the whole network and further the energy transfer involved in the luminescence.

The differences between the solid state and solution spectra of **9** (mixture of **9a** and **9b**) are analogous to the differences observed for other studied compounds (existing in the solid state as single polymorphic forms). Additionally the absorption/emission maxima visible in the solid state spectra of **9** do not show any effects suggesting that **9** is a physical mixture of **9a** and **9b** (which was proven by XRPD). This phenomenon originates from the character of the observed transitions. The emitting excited state of these compounds has an IL (intraligand) character. The electronic structure of the ligand is modified by participation of the ligand in the formation of the coordination bonds, but weak intermolecular interactions in the crystal lattice seem to have negligible effect on emissions of **9a** and **9b**.

Conclusions

The reactions of cadmium(II) nitrate with di-2-pyridyl ketone in the presence of pseudohalide (N_3^-, NCS^- and NCO^-) ions generated nine coordination compounds. The studies revealed that Cd^{2+} ions promote the conversion of the sp^2 hybridized C atom in $(py)_2CO$ to sp^3 $(py)_2C(OH)_2$ and $(py)_2C(OR)(OH)$. The inorganic anions not only balance the charges of the metal ion but also play a fundamental role in the formation of the final product and have a significant effect on its architecture. N_3^- and NCO^- ions facilitate the formation of tetranuclear cadmium compounds which are cubane-like structures, whereas the reactions of $Cd(NO_3)_2$, $(py)_2CO$ and NH_4SCN, which are dependent on the reaction variables, resulted in the formation of a helical 1D coordination polymer, a dimer as well as a cubane-like structure. The studies confirmed that the framework of dicubane-like cores in **5**, **7**, **8** and **9** is strongly reinforced by intramolecular O–H···N hydrogen bonds. Furthermore, the simultaneous presence of chelating nitrate and tridentate of organic ligands $(py)_2C(OH)(O)^-$ and $(py)_2C(OCH_3)(O)^-$ appears to promote heptacoordination of Cd(II) ions in **8** and **9**. Also, enhancement of fluorescence in the solid state compared to free ligand $(py)_2CO$ opens doors for new photochemical applications of these compounds, which are likely to be potential luminescent materials. One important advantage for the use of ligand-based emission in coordination compounds is that it may be tuned through variation of counteranions and/or the structure of the framework, as shown for the for examined compounds.

Acknowledgements

Iwona Nawrot is deeply grateful for the financial support of the "DoktoRIS – Scholarship program for innovative Silesia" co- financed by the European Union under the European Social Fund.

Notes and references

1 R. R. Osborne and W. R. McWhinnie, *J. Chem. Soc. A*, 1967, 2075–2078.

2 (*a*) A. C. Deveson, S. L. Heath, C. J. Harding and A. K. Powell, *J. Chem. Soc., Dalton Trans.*, 1996, 3173–3178; (*b*) O. J. Parker, S. L. Aubol and G. L. Breneman, *Polyhedron*, 2000, **19**, 623–626.

3 (*a*) Z. Serna, G. Barandika, R. Cortés, M. K. Urtiaga and M. I. Arriortua, *Polyhedron*, 1999, **18**, 249–255; (*b*) K. N. Crowder, S. J. Garcia, R. L. Burr, J. M. North, M. H. Wilson, B. L. Conley, P. E. Fanwick, P. S. White, K. D. Sienerth and Robert M. Graenger, *Inorg. Chem.*, 2004, **43**, 72–78; (*c*) A. Khutia, P. J. S. Miguel and B. Lippert, *Inorg. Chim. Acta*, 2010, **363**, 3048–3054; (*d*) H. Sartzi, C. C. Stoumpos, M. Giouli, I. I. Verginadis, S. Ch. Karkabounas, L. Cunha-Silva, A. Escuer and S. P. Perlepes, *Dalton Trans.*, 2012, **41**, 11984–11988; (*e*) F. A. Mautner, M. S. El Fallah, O. Roubeau, S. Speed, S. J. Teat and R. Vicente, *Eur. J. Inorg. Chem.*, 2013, 3483–3490.

4 (*a*) G. Yang, S.-L. Zheng, X.-M. Chen, H. Kay Lee, Z.-Y. Zhou and T. C. W. Mak, *Inorg. Chim. Acta*, 2000, **303**, 86–93; (*b*) E. Katsoulakou, N. Lalioti, C. P. Raptopoulou, A. Terzis, E. Manessi-Zoupa and S. P. Perlepes, *Inorg. Chem. Commun.*, 2002, **5**, 719–723; (*c*) A. J. Tasiopoulos and S. P. Perlepes, *Dalton Trans.*, 2008, 5537–5555; (*d*) Th. C. Stamatatos, C. G. Efthymiou, C. C. Stoumpos and S. P. Perlepes, *Eur. J. Inorg. Chem.*, 2009, 3361–3391; (*e*) J. C. Knight, A. J. Amoroso, P. G. Edwards, R. Prabaharan and N. Singh, *Dalton Trans.*, 2010, **39**, 8925–8936.

5 (*a*) Z. E. Serna, M. K. Urtiaga, M. G. Barandika, R. Cortés, S. Martin, L. Lezama, M. I. Arriortua and T. Rojo, *Inorg. Chem.*, 2001, **40**, 4550–4555; (*b*) G. S. Papaefstathiou, A. Escuer, F. A. Mautner, C. Raptopoulou, A. Terzis, S. P. Perlepes and R. Vicente, *Eur. J. Inorg. Chem.*, 2005, 879–893; (*c*) C. G. Efthymiou, C. P. Raptopoulou, A. Terzis, R. Boča, M. Korabic, J. Mrozinski, S. P. Perlepes and E. G. Bakalbassis, *Eur. J. Inorg. Chem.*, 2006, 2236–2252; (*d*) M.-Ch. Suen and J.-Ch. Wang, *Inorg. Chem. Commun.*, 2006, **9**, 478–481; (*e*) S. K. Padhi and R. Sahu, *Polyhedron*, 2008, **27**, 2662–2666; (*f*) C. C. Stoumpos, I. A. Gass, C. J. Milios, E. Kefalloniti, C. P. Raptopoulou, A. Terzis, N. Lalioti, E. K. Brechin and S. P. Perlepes, *Inorg. Chem. Commun.*, 2008, **11**, 196–202; (*g*) Z. Serna, N. De la Pinta, M. K. Urtiaga, L. Lezama, G. Madariaga, J. M. Clemente-Juan, E. Coronado and R. Cortés, *Inorg. Chem.*, 2010, **49**, 11541–11549; (*h*) E. Katsoulakou, V. Bekiari, C. P. Raptopoulou, A. Terzis, E. Manessi-Zoupa, A. Powell and S. P. Perlepes, *Inorg. Chem. Commun.*, 2011, **14**, 1057–1060; (*i*) C. J. Milios, P. Kyritsis, C. P. Raptopoulou, A. Terzis, R. Vicente, A. Escuer and S. P. Perlepes, *Dalton Trans.*, 2005, 501–511; (*j*) N. Lalioti, C. P. Raptopoulou, A. Terzis, A. E. Aliev, I. P. Gerothanassis, E. Manessi-Zoupa and S. P. Perlepes, *Angew. Chem., Int. Ed.*, 2001, **40**, 3211–3214; (*k*) A. K. Boudalis, Y. Sanakis, J. M. Clemente-Juan, B. Donnadieu, V. Nastopoulos, A. Mari, Y. Coppel, J.-P. Tuchagues and S. P. Perlepes, *Chem. – Eur. J.*, 2008, **14**, 2514–2526.

6 F. H. Allen, *Acta Crystallogr., Sect. B: Struct. Sci.*, 2002, **58**, 380–388.

7 Y.-M. Li, J.-L. Zhang and X.-W. Zhao, *Acta Crystallogr., Sect. E: Struct. Rep. Online*, 2007, **63**, m2475.

8 H.-G. Zhu, G. Yang and X.-M. Chen, *Acta Crystallogr., Sect. C: Cryst. Struct. Commun.*, 2000, **56**, 969–970.

9 M. Esmhosseini, N. Safari and V. Amani, *Acta Crystallogr., Sect. E: Struct. Rep. Online*, 2010, **66**, m1434–m1435.

10 *CrysAlis RED*, Oxford Diffraction Ltd., Version 1.171.35.11, 2011.

11 G. M. Sheldrick, *Acta Crystallogr., Sect. A: Found. Crystallogr.*, 2008, **64**, 112–122.

12 C. F. Macrae, I. J. Bruno, J. A. Chisholm, P. R. Edfinfton, P. McCabe, E. Pidcock, L. Rodriguez-Monge, R. Taylor, J. van de Streek and P. A. Wood, *J. Appl. Crystallogr.*, 2008, **41**, 466.

13 K. Nakamoto, *Infrared and Raman Spectra of Inorganic and Coordination Compounds*, 5th edn, John Wiley & Sons, Inc., New York, 1997.

14 H. D. Flack and G. Bernardinelli, *Chirality*, 2008, **20**, 681–690.

15 D. Bose, Sk H. Rahaman, R. Ghosh, G. Mostafa, J. Ribas, Ch.-H. Hung and B. K. Ghosh, *Polyhedron*, 2006, **25**, 645–653.

16 M. Cannas, G. Carta, A. Cristini and G. Marongiu, *Inorg. Chem.*, 1977, **16**, 228–230.

17 G. Mostafa, A. Mondal, I. R. Laskar, A. J. Welch and N. Ray Chaudhuri, *Acta Crystallogr., Sect. C: Cryst. Struct. Commun.*, 2000, **56**, 146–148.

18 M. Iwaoka and N. Isozumi, *Molecules*, 2012, **17**, 7266–7283.

19 Z.-L. You and H.-L. Zhu, *Acta Crystallogr., Sect. C: Cryst. Struct. Commun.*, 2005, **61**, m397–m399.

20 D. L. Reger, T. D. Wright, M. D. Smith, A. L. Rheingold, S. Kassel, T. Concolino and B. Rhagitan, *Polyhedron*, 2002, **21**, 1795–1807.

21 S. Ray, S. Konar, A. Jana, S. Jana, A. Patra, S. Chatterjee, J. A. Golen, A. L. Rheingold, S. S. Mandal and S. K. Kar, *Polyhedron*, 2012, **33**, 82–89.

22 S. Banerjee, B. Wu, P.-G. Lassahn, C. Janiak and A. Ghosh, *Inorg. Chim. Acta*, 2005, **358**, 535–544.

23 B. Machura, I. Nawrot and K. Michalik, *Polyhedron*, 2012, **31**, 548–557.

24 A. B. Caballero, A. Rodríguez-Diéguez, E. Barea, M. Quirós and J. M. Salas, *CrystEngComm*, 2010, **12**, 3038–3045.

25 M. Llunell, D. Casanova, J. Cirera, M. Bofill, P. Alemany, S. Alvarez, M. Pinsky and D. Avnir, *SHAPE program*, version 1.1b, Barcelona, 2003.

26 (*a*) D. Casanova, J. Cirera, M. Llunell, P. Alemany, D. Avnir and S. Alvarez, *J. Am. Chem. Soc.*, 2006, **126**, 1755–1763; (*b*) E. M. Zueva, E. R. Ryabikh and S. A. Borshch, *Inorg. Chem.*, 2011, **50**, 11143–11151.

27 G. J. Kleywegt, W. G. R. Wiesmeijer, G. J. Van Driel, W. L. Driessen, J. Reedijk and J. H. Noordik, *J. Chem. Soc., Dalton Trans.*, 1985, 2177–2184.